Active Flight Control and Appliqué Inceptor Concepts for Autorotation Performance Enhancement

Jeffrey D. Keller
Robert M. McKillip, Jr.
Continuum Dynamics, Inc.
Ewing, New Jersey

Joseph F. Horn
Thanan Yomchinda
Pennsylvania State University
University Park, Pennsylvania

ABSTRACT

Enhancing rotorcraft safety following engine or drive train failures has been a primary concern throughout the history of vertical flight operations. Previous work on autorotation trajectory optimization has shown potential for improved flight control and guidance solutions, and tactile cueing through active flight controls has been investigated to provide autorotation guidance without over-burdening the pilot during this high workload flight condition. This paper examines a notional autorotation tactile cueing system that follows an envelope limiting strategy for the entry, descent, flare, and landing phases to provide greater flexibility to the pilot. Methods for implementation of the guidance cues have been examined that range from adjustable stick force gradients (soft stops) to a surface-mounted appliqué device on the stick grip to provide localized unsteady tactile cues. The latter approach has been examined as a method to provide tactile cueing in legacy aircraft without active flight controls. The development and implementation of a collective axis cueing system is discussed, including supporting optimal autorotation trajectory and control analysis that was used as a design basis for cueing law development. Results are presented on the development and simulation of a prototype collective axis cueing system, development and bench testing of the appliqué cueing device, and pilot-in-the-loop simulation evaluations.

NOTATION

C_P	Rotor power coefficient
C_T	Rotor thrust coefficient
C_x	Rotor longitudinal force coefficient
C_z	Rotor vertical force coefficient
d	Downrange distance
ΔE_c	Autorotation energy margin limit parameter
f_e	Fuselage equivalent flat plate area
h	Wheel height above ground level
I_R	Rotor polar moment of inertia
J	Generalized cost function
J_p	Cost function performance term
P_s	Engine available (shaft) power
P_{res}	Residual engine power
u	Longitudinal velocity
$\mathbf{u}$	Control vector
$\mathbf{u}^*$	Optimal control vector
v_i	Rotor induced velocity
w	Vertical (descent) velocity
w_{crit}	Critical descent velocity at ground contact
$\mathbf{x}$	State vector
α	Rotor thrust tilt angle
δ_c	Collective stick position
$\delta_{c,ls}$	Collective cue lower stop position
$\delta_{c,us}$	Collective cue upper stop position
η	Engine propulsive efficiency factor
Ω	Rotor speed
Ω_{com}	Commanded rotor speed
τ_p	Engine power (droop) time constant

Presented at the American Helicopter Society 67th Annual Forum, Virginia Beach, VA, May 3-5, 2011.

INTRODUCTION

Helicopter propulsive and drive train system failures represent a critical operational condition potentially affecting safety of the aircrew and passengers. Survivability following a complete engine failure is strongly influenced by the ability of the pilot to quickly recognize the system failure and initiate an autorotation recovery. As an example, following an engine failure, the main rotor speed initially decreases until the pilot responds by reducing the main rotor collective pitch and the corresponding power/torque demand on the rotor. Excessive delay in pilot response can result in the rotor decelerating below the minimum safe rotational rate, leading to rotor stall and a potentially unrecoverable flight condition. Reductions in the stored kinetic energy in the rotor will also impact the terminal flare maneuver. Pilot training provides one avenue to enhance safety of helicopter autorotation, but autorotation success is also affected by other factors, including cockpit distractions and mission considerations.

Successful autorotation entry and recovery depend upon the helicopter configuration and flight condition at which engine, drive train, or tail rotor failure occurs. These characteristics are typically presented in terms of the height-velocity (H-V) diagram or "dead man's curve" (Figure 1 illustrates a representative H-V diagram), which provides a map of potential initial flight (autorotation entry) conditions where safe landing within the allowable helicopter limits may be achieved. Delay in initiating an autorotation entry, in particular for low altitude entries, may impact the ability to successfully perform the maneuver. A study of high speed autorotation entry characteristics has shown that modest delay times (between 1.5 and 2 seconds) can result in rotor speed excursions below the rotor stall limit for some helicopters [1]. Similar observations suggest that these findings are not only limited to high-speed flight but can also include other high power flight conditions, such as maximum gross weight hover and high speed climb.

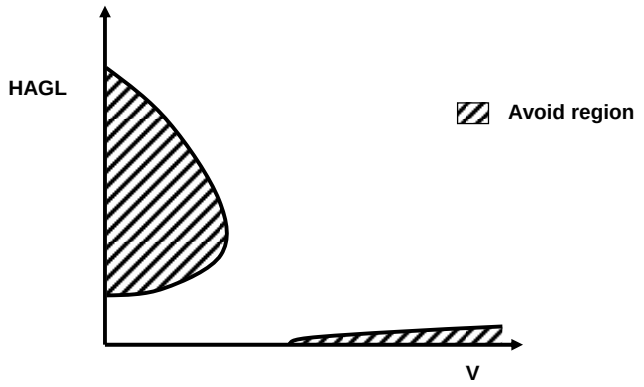

Figure 1. Representative Autorotation H-V Diagram Illustration

To improve helicopter autorotation execution and safety, solutions have been devised ranging from physical modifications to the rotor system to flight control and guidance strategies. Control and guidance solutions have focused on the use of trajectory optimization methods to minimize the terminal (landing) velocity following an engine loss at an initial altitude and flight speed. Many studies have been performed to define the optimal autorotation maneuver, as well as one engine inoperative (OEI) procedures, for conventional single-rotor helicopter configurations using a range of numerical solution procedures [2-9]. Similar studies have also been performed for multi-rotor (e.g., tiltrotor) aircraft configurations [10].

Recently, application of optimal trajectory/control analysis methods has been used to develop flight director guidance for assisting the pilot in performing an autorotation maneuver [11, 12]. In this previous work, the optimal control solution is determined as the aircraft performs flight operations, and following an engine failure, guidance commands are provided to the pilot through a flight director display that can assist in autorotation recovery. The flight guidance inputs can be used as a training aid or for performing automated autorotation recoveries. Demonstrations in piloted flight simulation studies for a Bell 206 helicopter have shown improvements in autorotation performance, including recoveries within the "avoid" region of the H-V diagram.

These prior studies have shown the potential benefit of optimal control strategies to improve autorotation performance, measured by the reduction of the "avoid" regions of the H-V diagram for a given aircraft configurations. While flight control and guidance methods may enhance autorotation safety, providing control guidance (cues) to the pilot in a manner that does not increase and preferably reduces workload is critical so that pilot attention can be focused out of the cockpit. Tactile cueing methods, through active flight control inceptors or other methods, provide one solution approach for cueing (optimal) control strategies to enhance autorotation execution. Tactile cueing methods have received much attention, in particular as a means to perform envelope protection and "carefree maneuvering", where tactile cues are used to provide feedback to the pilot on the proximity to performance limits so that these limits are not exceeded during aggressive maneuvering. Many studies have been performed examining the benefits of tactile cueing through active flight control/inceptor technology (examples of some previous work can be found in [13-19]). Tactile cueing using active inceptors has been pursued due to the benefit of providing unambiguous cueing to enhance handling qualities and reduce pilot workload, in addition to providing automatic flight control mode switching (regime recognition) based on how the pilot responded when encountering a tactile cue input [20, 21].

The present investigation described in the paper has focused on the application of tactile cueing methods to enhance autorotation execution (performance), and ultimately, safety. Given the previously demonstrated benefits of optimal control methods, an optimal trajectory analysis has been developed to provide a basis for the cueing

law implementation. The development and results presented herein have focused on the collective control axis, although the approach can be applied for other control axes. Evaluation of the autorotation guidance cueing laws have been performed using simulation, including a limited pilot-in-the-loop study performed in the Penn State University (PSU) Vertical Lift Research Center of Excellence (VLRCOE) rotorcraft simulation facility. In addition, initial development and testing of an appliqué tactile cueing device has been performed. This approach would allow tactile cueing to be used in legacy aircraft without active flight controls to enhance autorotation, as well as general handling qualities applications.

AUTOROTATION OPTIMAL TRAJECTORY ANALYSIS

This section provides an overview of the helicopter autorotation trajectory analysis, which is used as a basis for developing guidance cueing solutions. The governing equations of motion are presented first, followed by a discussion of the numerical solution procedure used in this study to define the optimal autorotation control strategy.

Autorotation Trajectory Equations of Motion

The equations of motion for autorotation optimal trajectory analysis for this study are similar to the model used in previous studies. The governing equations use a "point mass model" with additional degrees of freedom corresponding to rotor/drive train dynamics. This model formulation can be traced to Johnson [2], and variations of this model have been used in other prior work cited previously. Note that this model formulation has been compared against flight test data in some prior work, which has provided verification of the suitability of this model for use in trajectory analysis.

The point mass model formulation defines inertial frame longitudinal and vertical descent aircraft degrees of freedom, in addition to rotor speed and inflow states. To model engine torque/power train dynamics, an additional degree of freedom representing the available (shaft) power is included in the model. Control variables in this model are the rotor thrust magnitude and direction, which can be related to the collective and longitudinal cyclic control inputs. Figure 2 illustrates the aircraft degrees of freedom and control variables used in the analysis. The governing equations of motion are given as follows:

$$\dot{u} = \frac{1}{m}\left[\rho \pi R^2 (\Omega R)^2 C_x - \frac{1}{2}\rho u\left(u^2 + w^2\right)^{1/2} f_e\right] \quad (1)$$

$$\dot{w} = g - \frac{1}{m}\left[\rho \pi R^2 (\Omega R)^2 C_z + \frac{1}{2}\rho w\left(u^2 + w^2\right)^{1/2} f_e\right] \quad (2)$$

$$\dot{d} = u \quad (3)$$

$$\dot{h} = -w \quad (4)$$

$$\dot{\Omega} = \frac{1}{I_R \Omega} P_s - \frac{1}{\eta}\rho \pi R^2 (\Omega R)^2 \frac{R}{I_R} C_P \quad (5)$$

$$\dot{P}_s = \frac{1}{\tau_p}\left(P_{res} - P_s\right) \quad (6)$$

The aerodynamic coefficients C_X, C_Z, and C_P represent the non-dimensional rotor forces and power (torque) due to the rotor. The rotor force coefficients are related to the thrust coefficient and thrust tilt, which are taken as the control variables for the optimal trajectory analysis:

$$C_X = C_T \sin\alpha \quad (7)$$

$$C_Z = C_T \cos\alpha \quad (8)$$

The power (torque) coefficient C_P is approximated as follows:

$$C_P = \frac{1}{8}\sigma \bar{C}_d + C_T \lambda \quad (9)$$

where the non-dimensional rotor inflow parameter λ is given as follows:

$$\lambda = \frac{1}{\Omega R}\left(u \sin\alpha - w \cos\alpha + v_i\right) \quad (10)$$

and v_i is the rotor induced velocity.

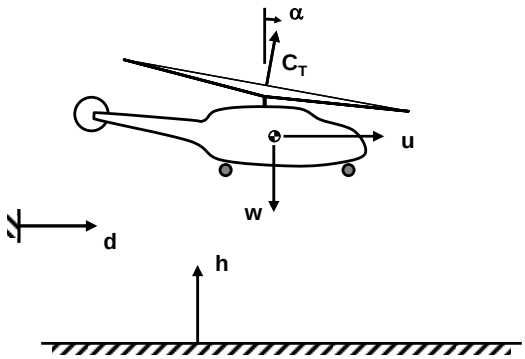

Figure 2. Helicopter Autorotation Analysis Point Mass Model Definitions

Modeling the induced velocity through the rotor requires additional consideration since the induced velocity has a strong impact on the rotor torque, and hence, the autorotation characteristics of a helicopter. An extension of simple momentum theory, based on the model used by Johnson [2], is used here (variations of this model have been used in previous studies as well). This model is mathematically represented as:

$$\dot{v}_i = \frac{1}{\tau_i}\left(K_{ind} f_I f_G v_h - v_i\right) \quad (11)$$

where

$$v_h = \Omega R\sqrt{\frac{C_T}{2}} \tag{12}$$

This model accounts for inflow dynamics and includes corrections for non-uniform inflow, vertical descent (power settling), and ground effects. Additional details for these inflow corrections are not reported here and can be found in other references (i.e., [2]).

The helicopter trajectory during autorotation can be found from the (initial value problem) solution of the nonlinear equations of motion, $\dot{\mathbf{x}} = \mathbf{f}(\mathbf{x},\mathbf{u})$, $\mathbf{x}(0) = \mathbf{x_0}$, which are described by Eq. 1 through 12. The state and control vectors are taken as follows:

$$\mathbf{x^T} = \begin{bmatrix} u & w & d & h & \Omega & v_i & P_S \end{bmatrix}$$
$$\mathbf{u^T} = \begin{bmatrix} C_T & \alpha \end{bmatrix} \tag{13}$$

Note that the control variables for this analysis do not correspond but can be related to the physical control inputs for the helicopter (i.e., collective and longitudinal cyclic stick inputs).

Optimal Autorotation Strategy

As noted previously, optimal control and trajectory analysis has been applied to the helicopter autorotation recovery problem. Mathematically, this problem is stated as follows: determine the control history $\mathbf{u}^*$ that minimizes the objective (cost) function J, i.e.,

$$\mathbf{u}^* = \min_{\mathbf{u}} J \tag{14}$$

subject to (inequality) constraints on the state vector $\mathbf{x}$ and control vector $\mathbf{u}$,

$$\mathbf{x_{min}} \le \mathbf{x} \le \mathbf{x_{max}}$$
$$\mathbf{u_{min}} \le \mathbf{u} \le \mathbf{u_{max}} \tag{15}$$

where the general form for the cost function is given as follows:

$$J = \frac{1}{2}Q_w w_f^2 + \frac{1}{2}Q_u u_f^2 + \frac{1}{2}\int_0^{t_f}\left(\dot{\mathbf{x}}^{\mathbf{T}}\mathbf{Q_S}\dot{\mathbf{x}} + \dot{\mathbf{u}}^{\mathbf{T}}\mathbf{Q_C}\dot{\mathbf{u}}\right)dt + J_p \tag{16}$$

In this generalized cost function, the terminal vertical and forward velocity components at landing (i.e., at the end of the autorotation maneuver corresponding to final time t_f) represent the primary performance metric for qualifying a successful autorotation. The integral term in the cost function has been included to "smooth" the optimal trajectory/control solution, as shown in previous work [12]. The final term (J_p) has been included as an additional "performance metric" in the cost function; this term will be discussed later in this paper in conjunction with optimal trajectory results.

Optimal Trajectory Solution Procedure

Previous studies of optimal autorotation trajectory and control strategies have applied a broad range of solution procedures and approaches for constraint handling. The approach adopted for this study is described below.

Control History Parameterization. Many previous studies have converted the optimal trajectory solution to a fixed parameter optimization by "re-parameterizing" the control histories. One approach re-parameterized the control time histories in terms of piecewise polynomial functions between collocation points (e.g., spline "knots"). For autorotation analysis, where the final time is not known a priori, this approach has been adapted in which the control strategy has been parameterized with respect to the helicopter height above ground. A similar approach was used by Johnson [2]. This approach is represented mathematically as follows:

$$u_i(h) = \sum_{j=1}^{N} u_i^{(j)} P\left(h; h^{(j)}\right) \tag{17}$$

where u_i is the ith component of the control vector; $u_i^{(j)}$ is the control value (parameter) for the ith control corresponding to the jth node, $h^{(j)}$ is the jth height node value, and $P\left(h; h^{(j)}\right)$ is an interpolating polynomial function. Note that several options are available for the interpolating polynomial function, and it has been found that better results are obtained using piecewise cubic Hermite functions.

Re-parameterizing the control histories with respect to height allows additional collocation points to be concentrated at critical segments of the autorotation maneuver (i.e., at autorotation entry and flare/landing phases). Alternatively, the height node values can be included as free parameters in the optimal solution. Use of free height node locations, in addition to the control values at those nodes, has been found to give better numerical results with a smaller number of control parameters, even though the addition of the node height values increases the dimension of the parameter vector space. Inclusion of free height nodes in the problem requires additional numerical considerations (constraints).

Solution of the helicopter trajectory has been found by performing a change in the independent variable from time to altitude. Doing so required that protection be placed on the vertical descent velocity to remain positive, thus preventing the governing equations from becoming singular. This restriction is not believed to be limiting since most

practical autorotation trajectories would not involve reversal in the vertical velocity direction during the maneuver. Since the resulting trajectory and control strategies are referenced to altitude using this solution procedure, it is necessary to using the following relationship:

$$t = \int_{h}^{h_i} \frac{d\tilde{h}}{w}, \quad 0 \le h < h_i \tag{18}$$

to provide "closure" to the optimal trajectory solution. This integral has been evaluated numerically and has been found to be well behaved given the above constraint on vertical velocity.

Solution Inequality Constraints. The autorotation optimal solution procedure has required the inclusion of inequality constraints to the state and control vectors. State and control constraints have been included corresponding to physical and operational limits of the helicopter. For example, limits to the rotor thrust coefficient and tilt were applied to reflect physical limits (e.g., rotor stall and allowable flapping excursions). Application of control constraints have been applied directly to the control-height node parameter values. While the interpolated control histories may exceed the limits due to overshoot in the interpolating polynomials, it was found that the use of cubic Hermite interpolating polynomials minimized this overshoot in contrast to other interpolating functions (such as cubic splines).

State constraints, such as minimum or maximum rotor speed excursions, have also been included in the optimization solution. These constraints were applied by definition of a general nonlinear constraint relationship $c_l(x_k) \le 0$ where

$$c_l(x_k) = \begin{cases} \max\left(x_k - x_{k,\max}\right) & \textit{upper lim} \\ \max\left(x_{k,\min} - x_k\right) & \textit{lower lim} \\ \max\left[-\left(x_{k,\min} - x_k\right)\left(x_k - x_{k,\max}\right)\right] & \textit{both} \end{cases} \tag{19}$$

Constraints have been applied to the forward velocity, descent velocity, and rotor speed following this nonlinear constraint relationship.

In addition, since the optimal trajectory solution used variable height node locations, it was found that inequality constraints were required to enforce a minimum spacing between neighboring height node values. These constraints were required to avoid numerical issues with the interpolating polynomial functions that could occur if neighboring height node values are nearly equal (or allowed to cross). These constraints can be defined in terms of a linear constraint equation, which can be readily incorporated into the numerical solution procedure.

Numerical Implementation. Numerical solution of the optimal autorotation trajectory and control strategy used a sequential quadratic programming (SGP) method. The numerical solution used numerical algorithms within the Matlab Optimization Toolbox. Numerical results presented in this paper used the free height node (trajectory collocation point) parameterization method, with a total of 7 collocation points for the trajectory. Parametric studies (not reported in this paper) indicated that this resolution was sufficient to provide good results.

Initial trajectory optimization results indicated that the numerical procedure was slow to converge, and this slow convergence was due to the cost function, which was found to be relatively "flat". Reduction of the relative thresholds used to define a numerically converged solution did not significantly reduce the number of iterations required for convergence, even though the solution and cost function did not vary significantly from iteration to iteration. An alternate convergence criterion was investigated in which convergence was based on the cost function change relative to a moving average. It was later determined that problems with slow convergence were attributed to the nature of the cost function that included only weights on the terminal velocity terms. Additional discussion is provided in the following section.

OPTIMAL TRAJECTORY RESULTS

Autorotation optimal trajectory and control solution results are presented in this section. Results are presented using model parameters representative of an H-60 class helicopter. Optimal autorotation trajectory/control solutions have been determined in which the helicopter was assumed to be in an initial (powered) trim condition and available engine power was immediately reduced to zero.

For all results presented herein, the following state and control limits were assumed:

$$\begin{aligned} &0.002 \le C_T \le 0.012 \\ &-20° \le \alpha \le 35° \\ &w \le 100 \text{ ft/sec} \\ &0.7\Omega_o \le \Omega \le 1.1\Omega_o \end{aligned} \tag{20}$$

where Ω_o is the 100% rotor speed value. Note that the rotor speed limits were chosen somewhat generously (the recommended power-off RPM range for the UH-60 is 90% to 105% with a transient limit of 110% as per the operator's manual). While use of a tighter set of bounds on rotor speed would likely result in higher terminal velocity conditions, it is not anticipated that the primary conclusions from this investigation will change.

Figures 3 and 4 illustrate optimal trajectory/control solutions for 500 feet above ground level (AGL) autorotation entries for different flight speeds and helicopter gross weights (16,000 and 21,000 lbs). In general, computed solutions qualitatively follow expected helicopter

autorotation characteristics. For example, low speed entries at this altitude represent the most challenging autorotation maneuvers, which should not be surprising since this region of the H-V diagram is most often recognized as "avoid" regions. The difficulty in obtaining satisfactory autorotation results for these entry conditions is reflected by the magnitude of the rotor speed droop during the maneuver.

Note that in almost all results using this analysis, the initial thrust coefficient (control) response counters conventional wisdom in which the collective pitch should be lowered immediately to initiate entry into a steady autorotation [22]. An immediate downward trend in the thrust coefficient, which is analogous to reducing the collective in this analysis, is only seen in the low speed, 500-foot entries. In other results, the optimal solution is seen to maintain or increase slightly the thrust coefficient relative to the level flight trim value. At this time, it is unclear if this solution artifact was caused by the model formulation or control parameterization approach.

One observation from the review of many optimal autorotation solutions was that a family of trajectory/control solutions can be found that have very nearly identical terminal velocity conditions but different trajectories, including final downrange distance. This observation should not be surprising since a pilot will alter his/her control strategy based on conditions not represented within the cost function (such as location of a suitable landing spot). To demonstrate this observation, a performance term (J_p) has been included in the general cost function defined in Eq. 16. This performance term can be used to account for other metrics (such as maximum range or endurance) when determining the optimal autorotation solution. Several options exist for this performance term:

$$\text{Max range:} \quad J_p = Q_p \left(\frac{d_{f,ref}}{d_f} \right) \tag{21}$$

$$\text{Min range:} \quad J_p = Q_p \left(\frac{d_f}{d_{f,ref}} \right) \tag{22}$$

In all of the above relationships, Q_p is the performance weighting factor and quantities denoted with the subscript "*ref*" represent normalizing reference quantities so the performance cost term, aside from the weighting factor, have approximately unit magnitude. Note that the objective of including these metrics for the present analysis is not to determine the best overall trajectory that balances both terminal constraints and overall performance. Instead, these metrics are used to permit qualitative comparison of trajectory solutions from a common entry condition. Moreover, it is unlikely that a trajectory devised using a minimum range metric would be useful beyond academic investigation in all but the most unique operational scenario.

Figures 5 and 6 illustrate the effect of a performance weight in the optimal autorotation cost function for the baseline helicopter (16,000 lbs gross weight) for 100 ft/sec entry conditions. Figure 5 illustrates the maximum range solution while Figure 6 illustrates the minimum range solution. Comparison of these results indicate that the overall range can be reduced (by 20%, 30%, and 50% corresponding to 500-ft, 1200-ft, and 2000-ft entry altitudes) with similar terminal velocity conditions. The important observation from these results is the primary condition affecting survivability of a particular autorotation maneuver (terminal velocity condition) can be satisfied through different (multiple) optimal control strategies. In some cases, other factors that may be important for successful autorotation execution are not readily related to the cost function formulation. Therefore, providing guidance based on a single optimal trajectory solution may be overly limiting.

Results focusing on the terminal segment (flare and landing) of the autorotation solutions are shown in Figure 6. These results were generated for the baseline helicopter (16,000 lbs gross weight) for 60 ft/sec autorotation entries (note that for one case, the helicopter was initially descending resulting in a higher rotor speed prior to initiating the collective flare). Trajectories have been plotted as a function of wheel height AGL. In these results (and most results using this analysis), the analysis has predicted the "collective pull" during the flare phase to result in a decrease in the rotor speed from the (approximately) steady state value during descent. The rate at which the rotor speed decreases during the (optimal) flare is approximately linear with altitude change. Shortly after initiation of this input, the rate of decrease of the descent velocity is seen to increase (in some cases slightly) until the aircraft is within 5 to 10 feet of the ground. At this point, ground effect becomes more important, and the rate of decrease of the descent velocity slows (and often increase slightly) as ground contact is made.

Optimal autorotation analysis results have yielded two notable observations: (1) a family of solutions may be obtained that satisfy terminal velocity constraints and (2) the terminal phase typically results in a linear variation in rotor speed as a function of wheel height AGL. These observations will be used in formulation of autorotation cueing strategies, described in the following section.

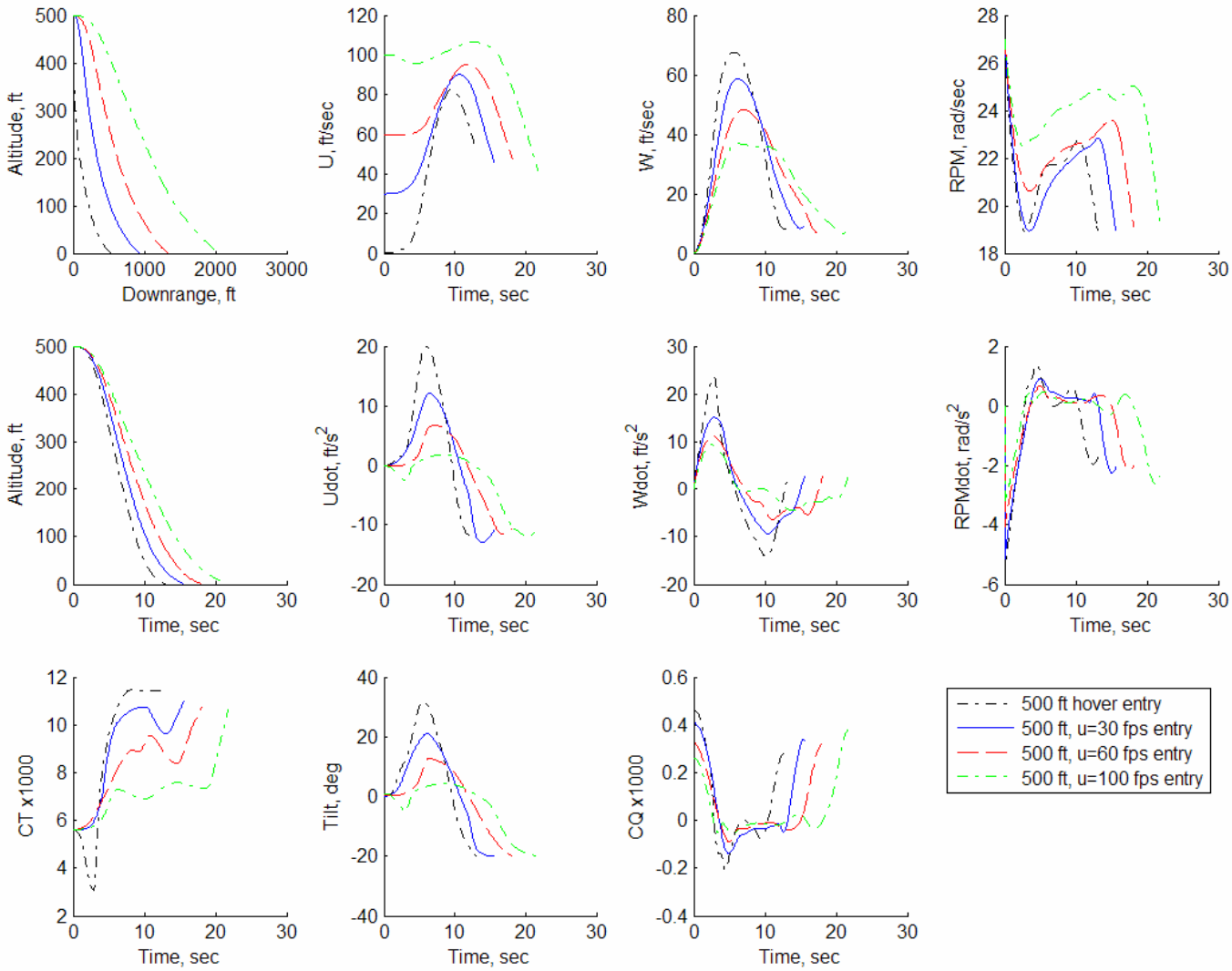

Figure 3. H-60 Optimal Autorotation Trajectory Results (16000 lbs gross weight; 500 ft altitude entry)

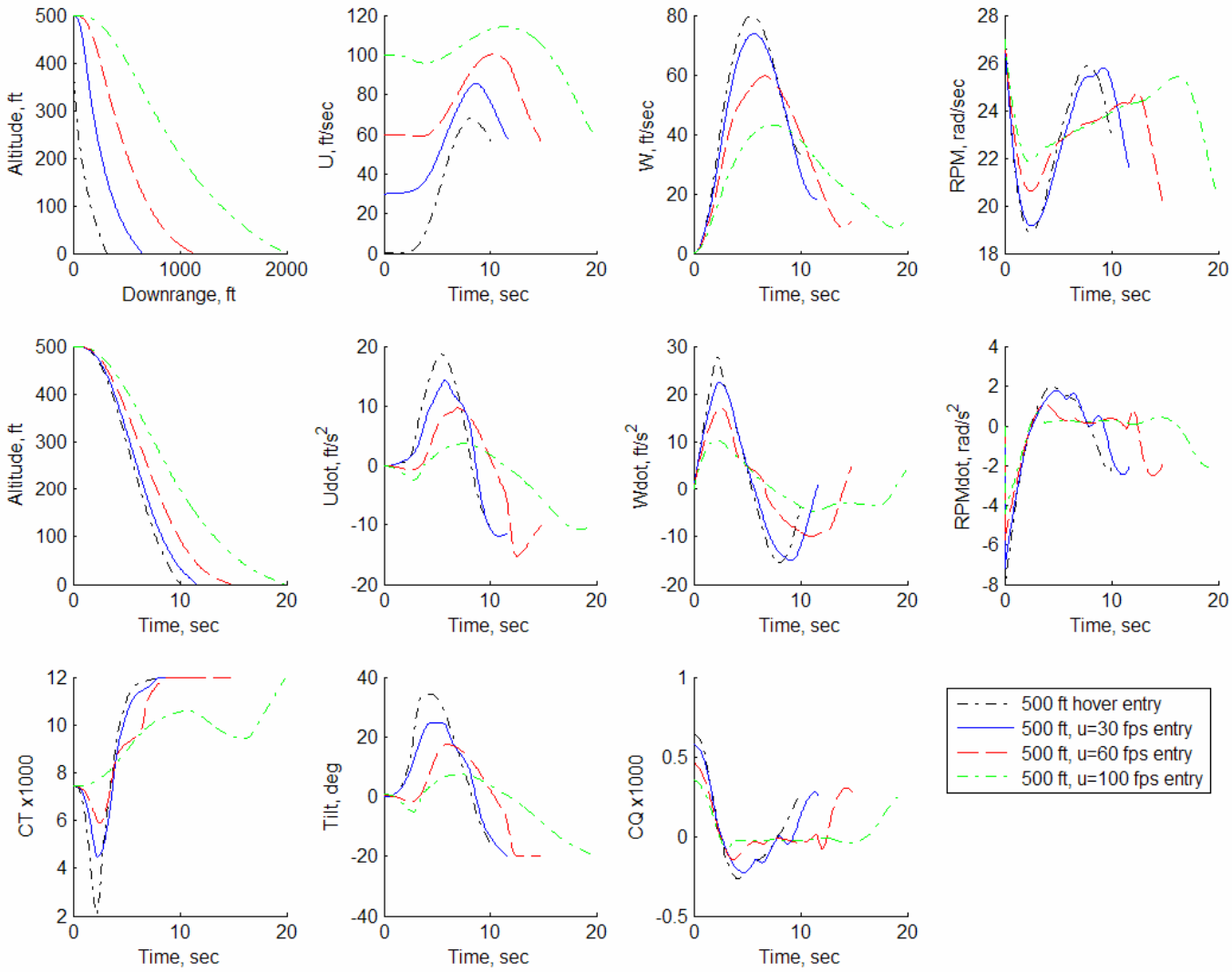

Figure 4. H-60 Optimal Autorotation Trajectory Results (21000 lbs gross weight; 500 ft altitude entry)

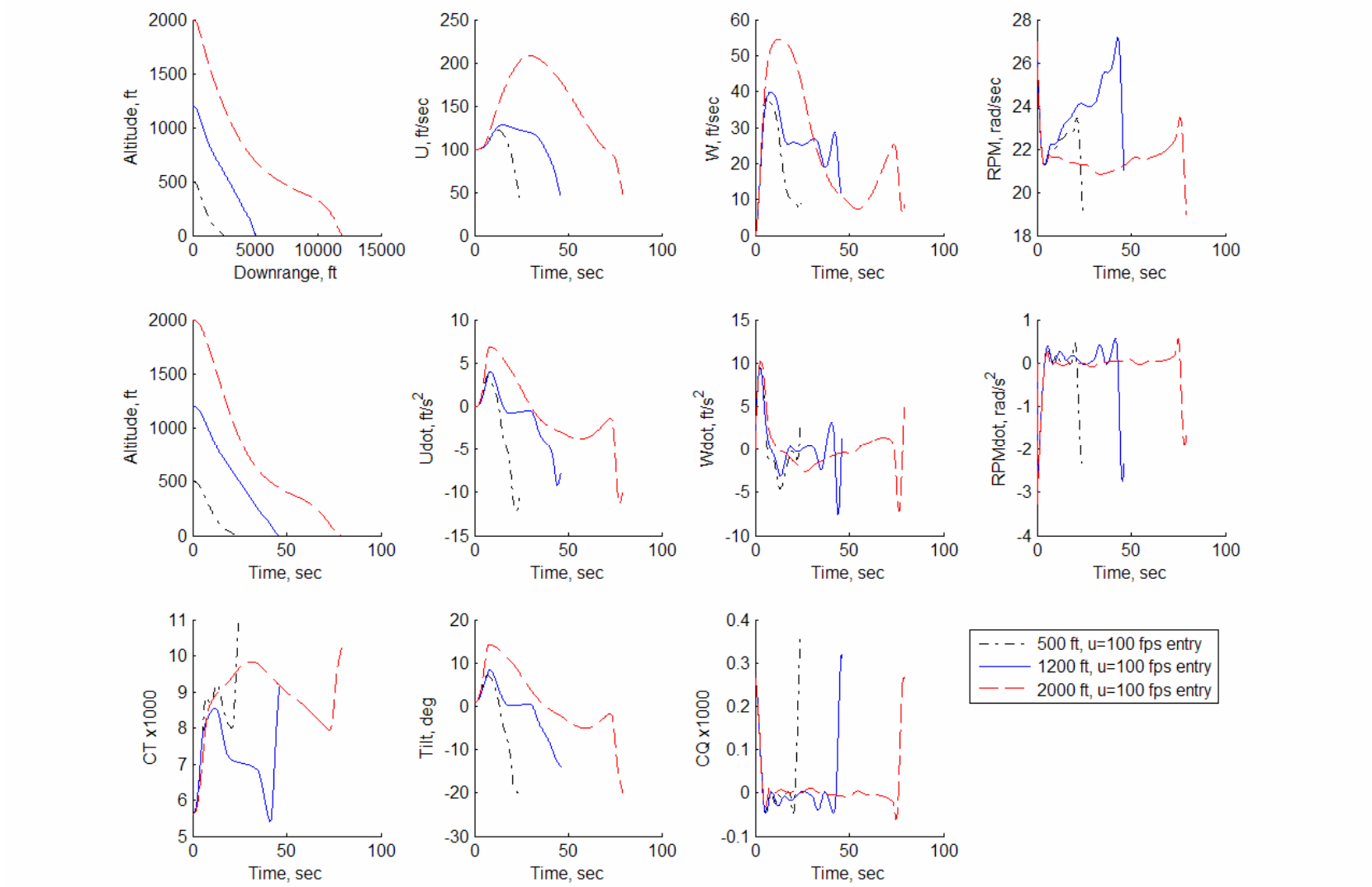

Figure 5. H-60 Optimal Autorotation Trajectory Results with Maximum Range Performance Weight (100 ft/sec forward speed entry condition)

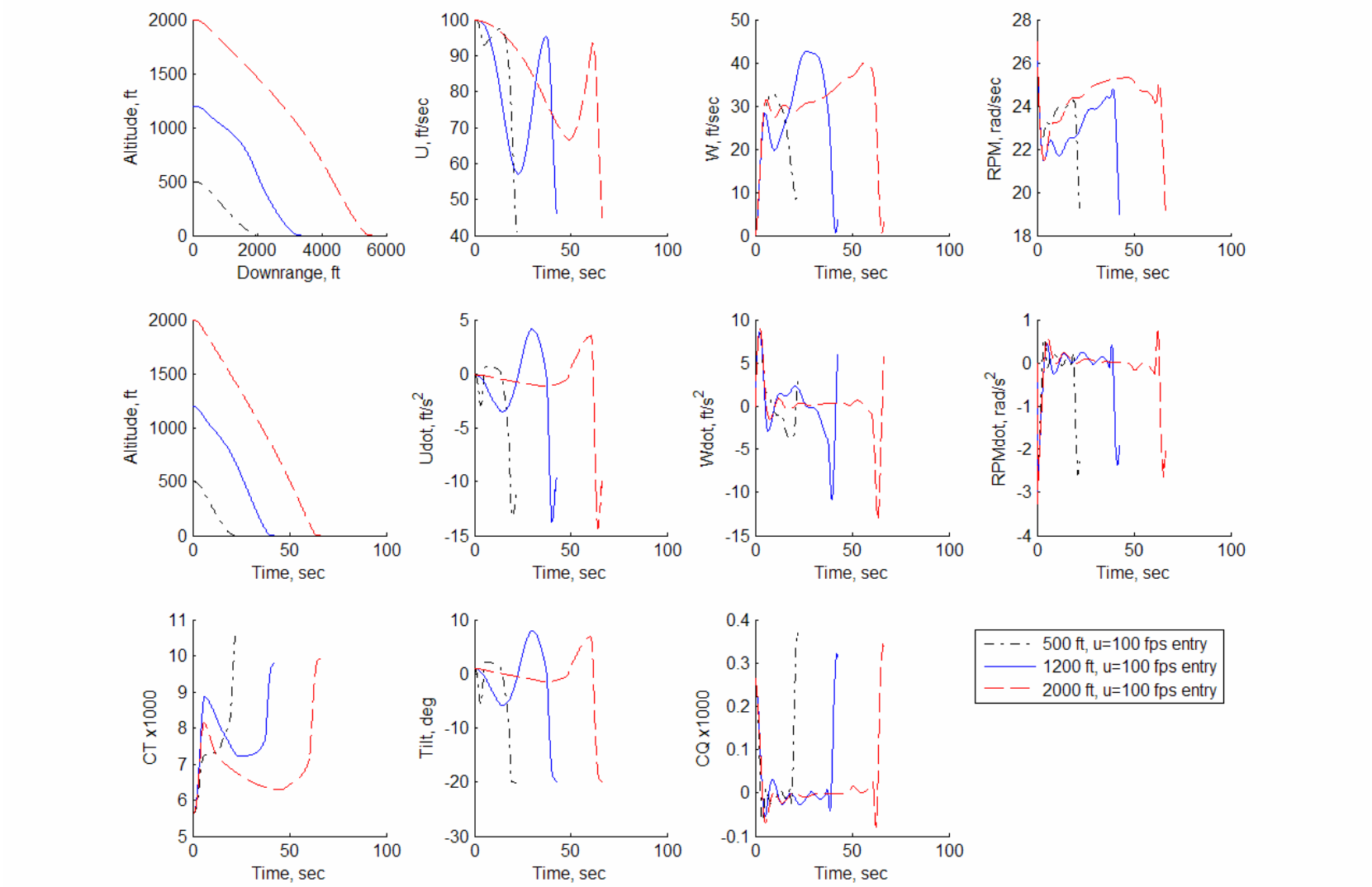

Figure 6. H-60 Optimal Autorotation Trajectory Results with Minimum Range Performance Weight (100 ft/sec forward speed entry condition)

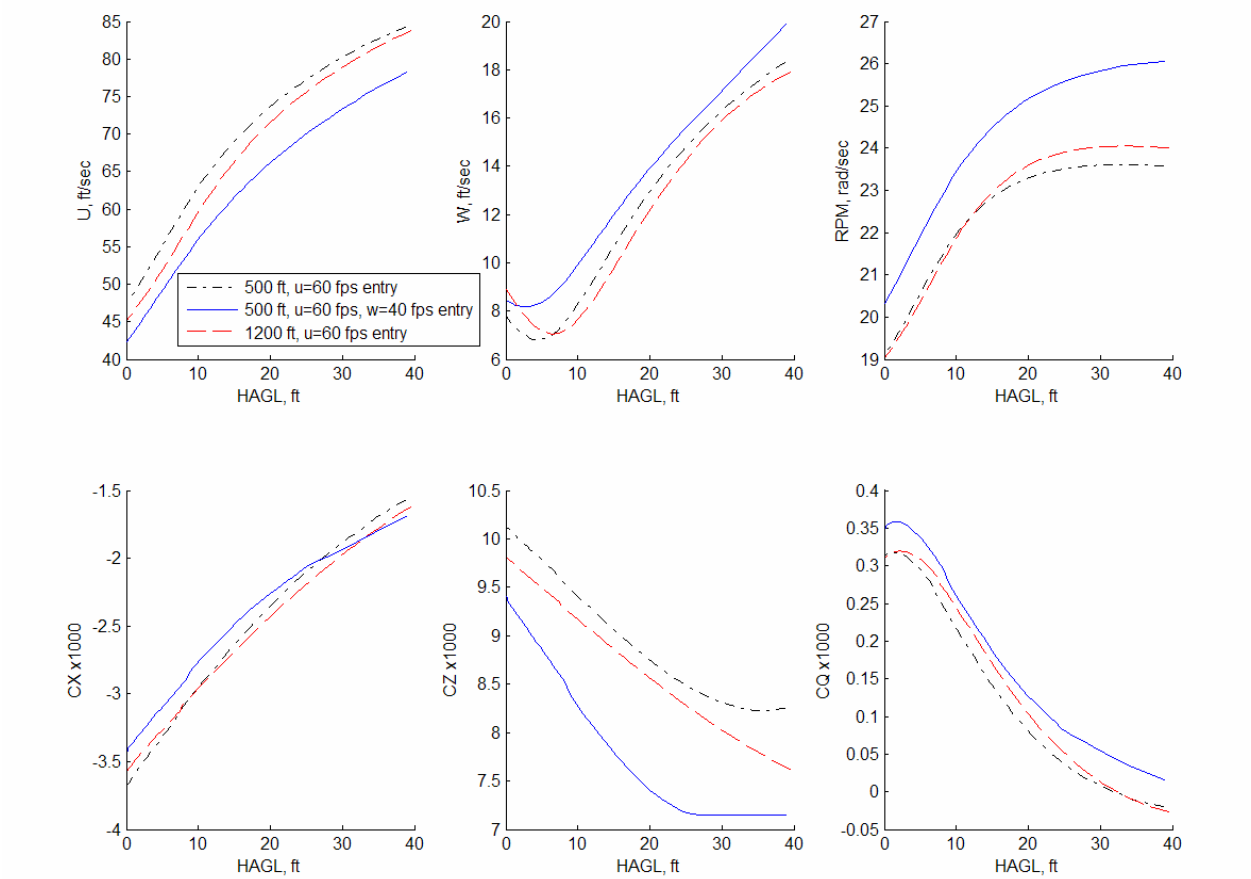

Figure 7. H-60 Optimal Autorotation Results for Flare Segment (16,000 lbs gross weight; 60 ft/sec forward speed entry conditions)

AUTOROTATION CUEING LAW DEVELOPMENT

A primary focus for the work described in this paper has been to identify and develop a tactile cueing strategy for aiding pilots during autorotation execution. Results from the optimal autorotation trajectory analysis have provided a basis under which this cueing strategy is developed. Given the trajectory analysis results described in the previous section, a cueing strategy that encourages the pilot to track a single optimal trajectory (either pre-computed or determined on-line based on the flight conditions when autorotation is initiated) appeared to be overly restrictive. Instead, an "envelope limiting" design approach has been used, in particular since multiple optimal solutions, which are driven by satisfying maximum terminal velocity criteria, may exist and be realizable from a given autorotation entry point. Furthermore, much experience has been gained from the use of tactile cues for envelope limit protection in non-autorotation applications, and thus, this prior work for tactile cue design and implementation can be applied here.

Following an envelope limiting approach to autorotation tactile cueing, a notional guidance cueing strategy has been investigated that included several distinct modes that depend upon the autorotation entry conditions. This notional design approach is illustrated in Figure 8, which maps the cueing strategy with respect to a generic helicopter H-V diagram. This schematic separates the cueing system implementation into three regions, corresponding to distinct flight control/cueing law modes that are enabled based on the helicopter state.

1. Baseline Autorotation Flight Control/Cueing Mode. The baseline control/cueing mode provides rotor speed limit protection centered on a rotor speed command (or alternatively vertical descent rate command) flight control mode. Since the primary requirement for most autorotation entry conditions is maintaining rotor speed between allowable limits, this cueing mode offers greater flight path freedom to the pilot while providing cues to protect against critical limit exceedances.

2. Autorotation Flare Control/Cueing Mode. Below a critical altitude, the autorotation cueing system switches to a flare mode in which direct guidance is provided to satisfy terminal velocity requirements at landing while maintaining other rotorcraft limits. This mode is developed to provide cues for execution of repeatable flare maneuvers.

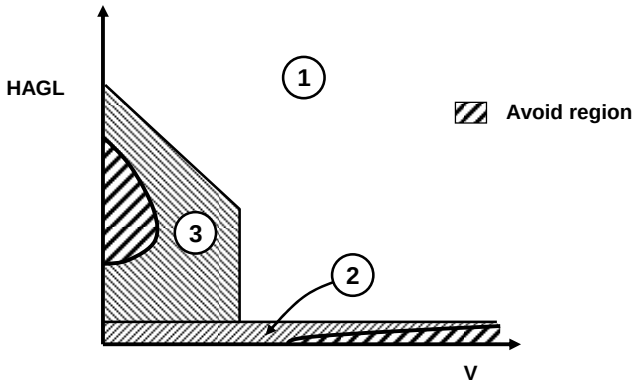

Figure 8. Schematic Illustration of Autorotation Flight Control/Cueing Law Modes Relative to H-V Diagram

3. Autorotation Guided Descent Control/Cueing Mode. For certain autorotation entry conditions (e.g., low altitude, low speed entries), it may be desirable to provide more direct guidance to the pilot given less margin exists for maintaining sufficient rotor speed prior to flare execution.

Developments described in this paper have focused on the baseline and flare cueing law applied to the collective control axis. A brief discussion of application to other control axes is provided later in this paper. Note that the guided descent mode more closely resembles a trajectory tracking strategy, although it is suggested that this guidance may be implemented using a variant on the baseline rotor speed command with tighter, height dependent limits.

Details of the baseline and flare collective axis guidance strategies are provided below. These guidance laws have been evaluated in simulation, with results presented in the remainder of the paper.

Baseline Autorotation Collective Axis Cueing Law

Analysis of autorotation trajectory and control strategies, in addition to previous work on autorotation safety enhancements, universally identify that maintaining sufficient energy in the rotor system (through control of rotor speed) is essential to safe autorotation execution. Recommended pilot techniques prior to the flare/landing phase also focus on ensuring that the rotor speed is controlled within acceptable limits of operation [22]. While optimal trajectory/control results have indicated that some (small) variation in the rotor speed may be beneficial, a common trend in the rotor speed histories from these results is that the rotor speed remains constant or increases slightly prior to the flare. Thus, a logical application of tactile cues in all autorotation phases is to maintain rotor speed within aircraft limits and to protect against excessive excursions. Note that a rotor speed limiting strategy also is compatible with autorotation entry requirements since the primary objective for transitioning from powered to autorotation flight conditions from an engine failure is to maintain rotor speed within allowable bounds.

While autorotation enhancement is not commonly addressed in previous studies of modern flight control applications, some studies have included an "autorotation mode" using a rotor speed command model [13, 18, 23]. This design approach has been used due to the greater sensitivity of rotor speed variations to collective inputs. An additional benefit of implementing a rotor speed command model is that the definition of the collective stick limits corresponding to allowable rotor speed margins is straightforward, following directly from the rotor speed-to-collective stick gain in the assumed command model. Thus, a rotor speed command model for the collective control axis has been used in the present study.

For the command model, perturbations in rotor rotational speed are commanded to be proportional to the collective stick input (δ_c) relative to the stick position corresponding to autorotation with 100% rotor speed ($\delta_{c,100}$), i.e.:

$$\begin{aligned} \Omega_{com} &= \Omega_o + \Delta\Omega_{com} \\ \Delta\Omega_{com} &= -K_\Omega\left(\delta_c - \delta_{c,100}\right) \end{aligned} \tag{23}$$

where Ω_o is the 100% rotor speed value and K_Ω is the collective stick-to-rotor speed gain. The collective stop lower and upper limits ($\delta_{c,ls}$ and $\delta_{c,us}$, respectively) providing rotor speed limiting are determined as follows:

$$\delta_{c,ls} = \delta_{c,100} - \frac{1}{K_\Omega}\left(\Omega_{\max} - \Omega_o\right) \tag{24}$$

$$\delta_{c,us} = \delta_{c,100} + \frac{1}{K_\Omega}\left(\Omega_o - \Omega_{\min}\right) \tag{25}$$

where $\Omega_{\min}$ and $\Omega_{\max}$ are the minimum and maximum allowable rotor speed excursions (during autorotation descent).

Several options may be used to implement the rotor speed command control/guidance law. For the results presented in this paper, a proportional-integral-derivative (PID) compensator was used. Gains for the PID controller were selected to minimize overshoot in rotor speed transients, and further gain tuning was performed as part of pilot-in-the-loop simulation evaluations.

Autorotation Collective Flare Cueing Law

Development of a collective flare cueing law to enhance the execution of repeatable flare maneuvers has been a primary focus of the present study. Following the envelope limiting design strategy, a cueing strategy was developed that factored in additional limits beyond rotor speed excursions. For autorotation flare execution, additional limits must be considered including physical aircraft limits

(i.e., vertical and forward terminal velocity, aft flapping), in addition to the ground proximity that provides a "hard limit" on the trajectory. It will be shown that the flare limiting cueing law will have the characteristics of an integral response type system [17, 24] in which the limit condition involves both the magnitude and timing of control application.

To develop the autorotation collective flare cueing law, it is recognized that the basic approach is similar to the roll rate command/bank angle limiting application described by Einthoven et al. [17]. This previous (albeit more straightforward) application, therefore, is used as a model for the present development. To outline the flare law development, the vertical response dynamics of a helicopter in autorotation is considered. This degree of freedom is governed by Eq. 2 in which the independent variable has been changed from time to altitude:

$$\dot{w} = -ww' = g - \frac{1}{m}\left[\rho \pi R^2 (\Omega R)^2 C_z + \frac{1}{2}\rho w\left(u^2 + w^2\right)^{1/2} f_e\right] \tag{26}$$

Note that the prime notation indicates differentiation with respect to altitude. Also, second term is small and can be neglected so that the governing equation can be written as:

$$ww' \cong c_1 \Omega^2 C_z - g \tag{27}$$

where

$$c_1 \equiv \frac{\rho \pi R^4}{m}$$

The limit condition can be found be integrating backwards from ground contact to a given altitude, where the corresponding velocity limit is taken as the maximum allowable descent velocity as supported by the landing gear (defined as w_{crit}). This velocity determines the allowable margin for safe autorotation landing (with respect to the vertical degree of freedom). Integrating and rearranging yields the following:

$$\Delta E_C \equiv \frac{1}{2}\left(w^2 - w_{crit}^2\right) + gh = \int_0^h c_1 \Omega^2 C_z d\tilde{h} \tag{28}$$

which represents the fundamental relationship for the primary limit parameter (i.e., the proximity of the current energy state of the helicopter relative to the required state at touchdown) that will be used to define the cueing input to the pilot. Note that the expression given in Eq. 28 is analogous to the bank angle integral limit criterion given by Einthoven et al. (i.e., Eq. h5 in [17]). Evaluation of the integral term on the right hand side of Eq. 28 is more complicated, however, since this fundamental limit relationship is derived from the dynamic equation of motion governing the vertical motion degree of freedom rather than the much simpler kinematic relationship between roll angle and roll rate.

The collective flare cueing law can be derived by evaluating the integral term on the right hand side of Eq. 28 in terms of a prescribed collective stick input (stop), which then is inverted to relate the stick (stop) motion to the primary limit parameter. To evaluate the integral term in Eq. 28, it is necessary relate the integrand to pilot control inputs. Again, following from the approach outlined in [17], an assumed collective stick "program" is used for the flare maneuver. Several options can be used for the collective stick program as follows:

$$\delta_c = \delta_{c,ls} = c_f\left(t - t_f\right) + \delta_{c,100} \tag{29a}$$

$$\delta_c = \delta_{c,ls} = c_f\left(h_f - h\right) + \delta_{c,100} \tag{29b}$$

where t_f and h_f are the flare initiation time and altitude, respectively (i.e., the point at which the autorotation flare cueing law is enabled), and c_f is the rate of travel of the collective stick (stop) during the flare. Since the autorotation flare involves a collective stick pull (corresponding to a decrease in rotor speed as energy is transferred from the rotor to arrest the descent rate prior to touchdown), this collective stick program is used to drive the lower collective stop $\delta_{c,ls}$. An altitude-referenced collective stick program (Eq. 29b) versus a time-referenced program has been used for the cueing law development, which is believed to provide a more "natural" motion of the collective stick.

In addition, selection of the height-referenced program implies that the collective pull during the flare approximates the optimal flare solution, when perturbations in the rotor speed are commanded to be proportional to the collective stick deflection (i.e., as for a rotor speed command flight control system). This implication is supported by the optimal trajectory results presented previously. Thus, Eq. 29b provides an approximate representation of the optimal collective control input for the autorotation flare.

Given the rotor speed command model used in the baseline autorotation flight control law (Eq. 23), the height-referenced collective stick program (Eq. 29b) can be used to define the (commanded) variation in rotor speed as a function of altitude. To evaluate the right hand side of Eq. 28, it is also necessary to define the vertical force coefficient as a function of altitude, which is more complicated since in general $C_z = C_z(\delta_c, w, u)$ where δ_c, w, and u vary with altitude. It is possible to develop a closed-form cueing law relationship if the following approximation is made:

$$C_z = C_{z,ave} = \text{ constant}$$

Optimal trajectory analysis results suggest that this approximation may be reasonable in some cases. From an

implementation perspective, selection of an appropriate value for $C_{z,ave}$ may be determined (empirically) from engineering simulation studies. Note that simulation results were used to determine a suitable average value. Alternatively, development of a higher-order predictive methodology for the vertical force coefficient, for example, using a regression or neural network model, can be used in the implementation of the cueing law. This aspect was not investigated and may be considered in future work.

To complete the derivation of the autorotation cueing law, a "closure condition" is required that is used to relate the parameters in the collective stick program to physical limits on the desired stick travel. This condition is determined based on the collective position at the end of the flare ($h = 0$):

$$\delta_c(h=0) = \delta_{c,100} + c_f h_f = \delta_{c,m} \tag{30}$$

where $\delta_{c,m}$ is the maximum collective stick deflection. Ideally, this maximum deflection should be limited to no more than the maximum collective stick travel less some margin to permit the pilot to pull through the stop if necessary. Given the rotor speed command model, the maximum collective stick can be related to the minimum rotor speed allowed during the terminal flare. i.e.,

$$\Omega_{\min} = \Omega(\delta_{c,m}) = \Omega_o - K_\Omega(\delta_{c,m} - \delta_{c,100}) \tag{31}$$

Given the above assumptions and restrictions, it is possible to reduce the autorotation collective flare cueing law to a closed-form expression. In this case, Eq. 28 reduces to a cubic polynomial that will have one real solution and two complex conjugate roots. Algebraic details of this derivation are omitted; the single real solution yields the collective flare cueing law:

$$\delta_{c,ls} = \delta_{c,m} + \frac{\Omega_{\min}}{K_\Omega}\left[1 - \left(1 + 3\frac{c_f K_\Omega \Delta E_c}{c_1 C_{z,ave} \Omega_{\min}^3}\right)^{1/3}\right] \tag{32}$$

It has been found that the collective lower stop cueing is proportional to the cube root of the helicopter energy state limit parameter (ΔE_c). All other terms in the cueing law represent control system/design parameters (except for the parameters c_1, which is a physical parameter for a given helicopter, and $\Omega_{\min}$, which is an aircraft-specific limit).

Tactile Cue Generation

The autorotation tactile cueing system development separated the cueing law design from the method(s) used to present guidance to the pilot (tactile cue generation). For the latter, several options were considered as part of pilot-in-the-loop simulations (note that the nature of the cue type – quasi-steady or unsteady – is also indicated):

- Force bias/trim offset (quasi-steady)
- Variable spring gradients (quasi-steady)
- Movable soft stop/nonlinear stick force gradients (quasi-steady)
- Stick shakers (unsteady)
- Stick pulsers (unsteady)

Both steady and unsteady methods have been used in previous applications of tactile cues for rotorcraft limit/envelope protection. Sahasrabudhe et al. [18] demonstrated through simulation studies that both quasi-steady (soft stops) and unsteady (stick shakers) tactile cueing methods can be effective, and furthermore, provide the ability to cue multiple limits through a single (collective) axis.

In piloted simulation studies, both soft stops and stick shakers were used to provide autorotation descent (rotor speed command/limiting) and flare guidance to the pilot. The stick shaker cue was used to simulate a retrofit tactile cueing concept that was investigated as part of this study to provide the ability to "retrofit" legacy (non-active) flight control systems. As noted previously, this aspect of the research and development was pursued to permit the application of tactile cueing guidance to legacy aircraft without active flight control systems. Note that the actual stick shaker cue implemented in piloted simulations also included a bias force (weak stick gradient) to provide directionality cues that are present in the retrofit concept. Additional details for this retrofit concept are presented later in this paper.

Multi-axis Cueing Law Extensions

The above approach used for the development of the collective flare cueing law also may be applied to the cyclic flare maneuver, thus providing a multi-axis cueing system for repeatable execution of the terminal phase of the autorotation maneuver. For the longitudinal axis, the fundamental limit-parameter-control relationship (analogous to Eq. 28) will depend on the difference between the current and critical forward velocity with further limits due to maximum allowable rotor flapping and nose-up pitch attitude. Given the nature of the governing dynamic relationships, the longitudinal axis cueing law will depend on the vertical degrees of freedom, in contrast to the collective axis that can be approximately decoupled.

ENGINEERING SIMULATION EVALUATION

Evaluation of the cueing laws was performed using engineering simulation as a precursor to piloted simulation evaluations. These simulations were used to verify the cueing system architecture and to refine cueing laws (gain tuning) prior to pilot-in-the-loop evaluations. Simulations were performed assuming "perfect tracking" of the tactile cues to the pilot (i.e., the pilot recognizes and tracks the cues perfectly).

Example engineering simulation results are shown in Figure 9, which illustrate the response starting from a 50 ft/sec descent velocity and 100 feet AGL. During the initial segment of the simulation, the baseline flight/control cueing mode is enabled, so that the collective control is commanding rotor speed. The rotor speed command model is designed so that 1-inch of collective stick deflection corresponds to autorotation at 100% RPM, and the stick-rotor speed gearing is chosen so that minimum rotor speed occurs with stick deflection of approximately 9 inches. The collective flare cueing law (Eq. 32) is calculated continuously but only enabled at 20 feet AGL. The motion of the collective lower stop forces the pilot stick position to be increased following "perfect" cue tracking. Note that the $C_{z,ave}$ parameter in the flare cueing law was determined empirically, providing a "gain tuning" parameter.

For reference, results from the optimal autorotation trajectory analysis are compared with the baseline/flare cueing law simulation. Optimal trajectory results shown in Figure 9 correspond to the baseline (16,000 lbs) H-60 for an autorotation entry from 60 ft/sec forward speed, 40 ft/sec descent rate, and 500 feet HAGL. The optimal trajectory is seen to have a lower initial but higher average descent velocity over the simulation duration. The optimal rotor speed profile (plotted versus height AGL) matches well with the commanded rotor speed flare profile, which provides a decrease in the commanded rotor speed proportional to the change in altitude.

Additional closed-loop (perfect tracking) simulation results are shown in Figure 10. These results correspond to an updated implementation of the collective flare cueing law following additional gain adjustment. Results are shown for an autorotation entry altitude of 300 feet and different entry velocities. In each simulated case, the collective axis cueing law provides commands to arrest the descent rate with better performance (lower terminal descent velocity) with higher forward speed. For these cases, the time of the minimum descent velocity occurs just before ground contact, which occurs since the cueing law has driven the lower stop position to command the minimum allowed rotor speed, at which point the collective stick position is held fixed. At this point in the simulations, the rotor speed controller proceeds to reduce the collective pitch input to the rotor, which reduces thrust and hence increases the descent rate. Further refinements to the rotor speed controller may eliminate this behavior, but these refinements were not performed prior to piloted simulations.

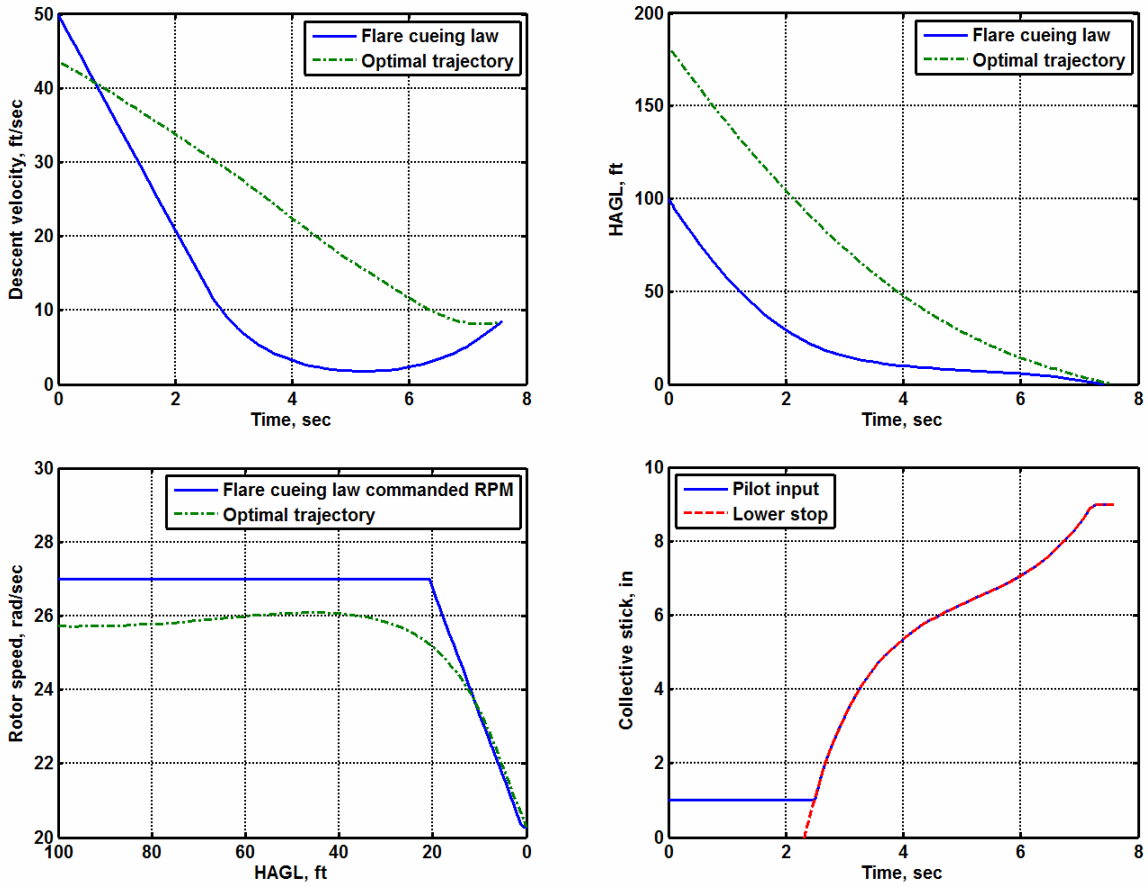

Figure 9. Comparison of Engineering Simulation Evaluation of the Baseline/Flare Autorotation Cueing Law with Optimal Trajectory Solution Results

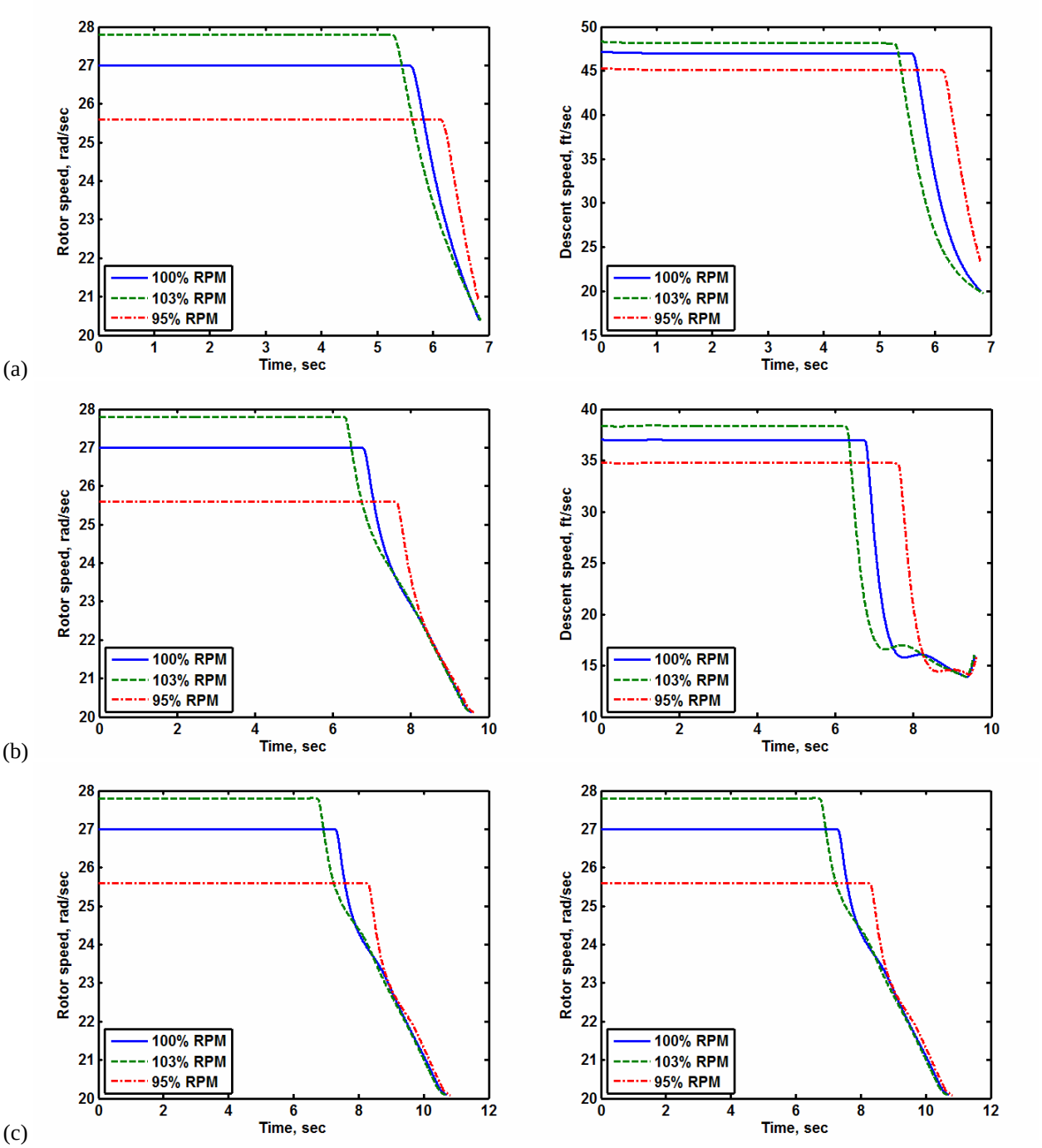

Figure 10. Closed-loop Simulation Evaluation of Collective Axis Flare Cueing Law from Steady Autorotation: (a) 50 ft/sec entry, (b) 80 ft/sec entry, (c) 100 ft/sec entry

Simulation results presented in Figure 10 were generated assuming no cyclic input, i.e., the thrust tilt was maintained at the trim value and the forward speed was unchanged during the autorotation. Results have also been generated in which a representative "cyclic flare" was applied (open loop) while the collective axis was driven by the cueing law. It was found that the cyclic input had little effect on the autorotation vertical axis performance based on simulation results using the point mass model. Further assessment of this finding has been examined in piloted simulations.

PILOTED SIMULATION EVALUATION

Pilot-in-the-loop simulations were performed to evaluate the autorotation tactile cueing strategy, including force cue generation methods. These simulations were limited in scope due to preliminary nature of the study but

provided useful feedback for future developments. A description of the simulation facility, test approach, and results are summarized below.

Penn State Piloted Simulation Facility

Evaluation of autorotation flight control and tactile cueing concepts was performed in the Penn State University (PSU) Vertical Lift Research Center of Excellence (VLRCOE) rotorcraft simulation facility. The PSU simulation laboratory (Figure 11) is built around a donated XV-15 simulation cab that includes a programmable electromechanical control loading system, components of the original XV-15 cockpit, realistic control inceptors, and a variety of programmable switches. The simulator includes a three-channel image generation system projected onto a 15-ft diameter, 11-ft high, 180° field of view screen and flat panel instrument displays. All components of the simulator (math model, image generation, cab communication, displays, control loading, etc.) are connected via a local network, such that the computational load is distributed over up to 8 separate PC computers.

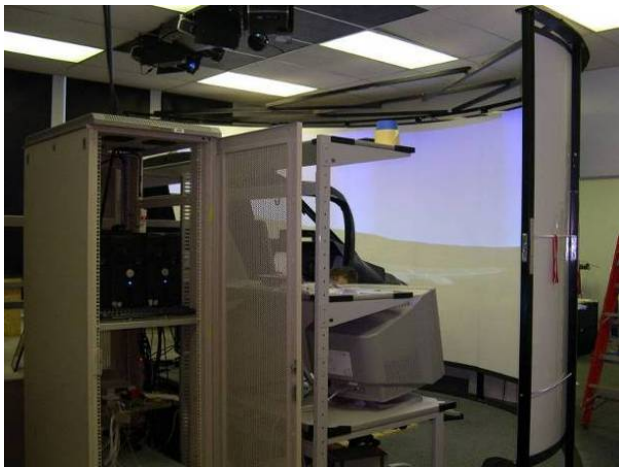

Figure 11. PSU VLRCOE Simulation Facility

The GenHel-PSU software was developed at Penn State University for use in basic research on rotorcraft flight dynamics and control [25]. It uses a modified version of the U.S. Army GenHel model [26], which is a non-linear, blade element flight dynamics model that has been used in many handling qualities and flight control studies over the last 20 years. Much of the basic GenHel flight dynamics model has not been significantly modified, but the GenHel-PSU code includes some added functionality: an interface with the MATLAB / Simulink software environment; the capability to generate high order linearized models; and the capability to include user defined control laws for roll, pitch, yaw, collective, and rotor RPM in place of the existing UH-60A mechanical control system, stability augmentation systems (SAS), and engine electric control unit (ECU).

GenHel-PSU has also been integrated with the CHARM free wake module to provide higher fidelity modeling of the main rotor inflow. This enhanced rotor induced velocity model is especially critical for accurate modeling of descending flight conditions and ground effect during the flare maneuvers. The CHARM wake is executable in real-time in the GenHel-PSU simulation code [27].

Collective axis control/cueing laws described previously were implemented in the simulation in Simulink and transitioned directly to the simulation software using Real-Time Workshop (RTW), providing an efficient "pictures-to-code" development environment. Figure 12 shows a sample portion of the Simulink diagrams used to model the collective axis autorotation control law and cueing law used in this study. The overall control diagram is compiled using RTW and linked to the GenHel-PSU code as a dynamic link library (DLL). In this manner, control and cueing parameters can readily be modified, compiled, and tested in the real-time simulator with a turn-around-time of less than 1 minute. This capability proved to be very useful for the testing conducted during this preliminary study and would provide an essential capability as algorithms are further refined in future work.

For the remaining control axes, existing advanced control laws were used so that issues in the other axes do not over shadow any changes in handling qualities associated with the collective axis. An existing baseline model-following control law was used to achieve attitude command / attitude hold (ACAH) response type in pitch and roll and a rate command heading hold (RCHH) / turn coordination (TC) response type in yaw [28]. The baseline collective axis is a simple "stick-to-head" control of the main rotor collective pitch. Collective control can then be toggled to the autorotation control law after engine failures. Pilot switches were used to engage or disengage the autorotation control and cueing algorithms. A switch on the co-pilot collective lever was used to initiate a simulated engine failure. This switch is tied to a flag in GenHel-PSU that instantaneously disables both engines.

The PSU VLRCOE simulator cab features a fully programmable Fokker control loading system. The control loading system allows dynamic changes to be made to the force characteristics of all primary control inceptors. The systems allows for a multi-segmented piecewise linear force feel curve (multiple gradients), which permits implementation dynamic soft stop cues (although the secondary gradient is not simulated within the current programming framework). The system also allows for variable frequency and variable amplitude stick shaking cues. The GenHel-PSU software and the interface to the control loading system were modified to allow cues to be communicated from the control laws to the control loading system. Data input/output between the control loaders and host computer are transferred at a 20 Hz update rate. Testing showed that the simulator could provide clear force cues to the pilot based on the current state information on the aircraft.

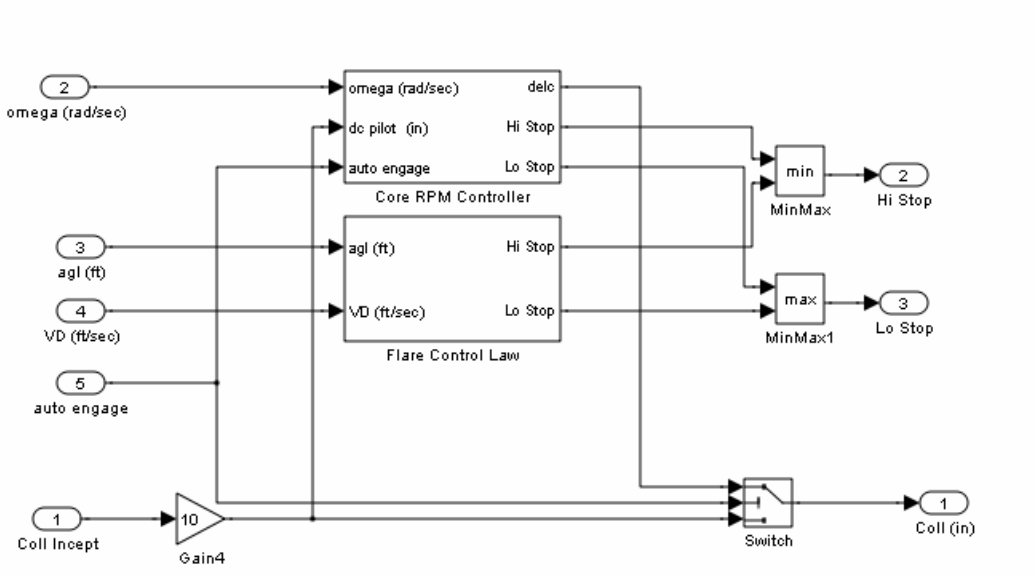

Figure 12. Simulink Diagram for Collective Axis Control Law Used in Simulation Study

Piloted Simulation Study Plan

The piloted simulation study was performed to provide a preliminary evaluation of the autorotation collective axis cueing system. Specific objectives included: implementation of prototype collective axis control and tactile cueing algorithms in a representative simulator; evaluation of these algorithms with respect to autorotation performance (execution) enhancement; and evaluation of tactile cueing methods (gradient/soft stop versus stick shaking). It was recognized that available resources for the investigation precluded a formal handling qualities study to be performed, thus the primary outcome sought was more "qualitative" in nature to guide future developments. A test approach, however, was developed that mimicked features of a formal handling qualities study.

Simulation evaluations were performed with two pilots: a former test pilot on staff (Pilot A) and an engineer with extensive UH-60 simulator familiarity (Pilot B). Pilot A served as the primary evaluation pilot. At the time of the study, Pilot A had approximately 1200 hours flight time and 500 hours simulator time, primarily in UH-1 helicopters with most UH-60 experience in simulators. Feedback from Pilot B was used primarily to supplement results from Pilot A.

Prior to autorotation tactile cueing law evaluations, pre-test shakedown was performed to refine cueing law gains and force generation parameters. This pre-test shakedown was also used to allow the test pilot time for familiarization with the baseline aircraft flight dynamics. This familiarization flight consisted of level flight, climb, descent, in-ground effect (IGE) flight, and landing, as well as several practice autorotations. Pilot comments during this part of the evaluation indicated that both power-on and power-off autorotations "seemed reasonable", although it was commented that visual cues were slightly limited and could benefit from an increase in the vertical field of view.

Collective axis control/cueing laws evaluations were then performed following a pre-defined test procedure:

1. An initial powered flight trim condition was established downrange from an airfield. The test pilot engaged the collective axis control/cueing laws (based on the test condition) and enabled the flight data logger using cockpit switches.
2. Engine power was cut by the test engineer (using a separate switch at the copilot seat). The pilot performed an autorotation entry and maintained a steady descent condition with rotor speed within desired limits (90% to 103% RPM) during descent. Autorotation maneuvers were performed with minimal lateral-directional flight path variations (straight-in autorotation).
3. The autorotation flare and landing were performed to minimize the forward and vertical (descent) velocity at ground contact (rotor speed was allowed droop below the lower limit for descent). Note that the simulation was frozen when the gear contacted the ground so that the terminal velocity conditions could be recorded.

A snapshot from one autorotation test flight is shown in Figure 13, showing the out-the-world view from the cockpit during the descent phase of one simulated autorotation maneuver. The test procedure outlined above was repeated multiple times without and with collective axis control/cueing laws enabled. Although it was originally planned to perform evaluations at different entry conditions, it was found that sufficient "scatter" in the overall performance was present so that multiple repeat tests at the

same entry condition were needed to allow some degree of statistical treatment of the simulation results.

Figure 13. Snapshot of Out-the-window View from Piloted Simulation Evaluation of Autorotation Collective Axis Tactile Cueing Law

Piloted Simulation Results

Results from piloted simulation evaluations of the prototype collective axis tactile cueing system are presented here. All simulated autorotations were performed from an initial level flight (entry) condition of approximately 60 knots forward speed and 1000 to 1200 feet AGL. The gross weight of the UH-60A helicopter was 16,820 lbs for all cases simulated, which is slightly larger than the design point for the collective axis control/cueing laws (baseline gross weight of 15,870 lbs). Simulations were performed with collective axis control/cueing laws disabled; with collective axis cueing using variable soft stops; and with collective axis cueing using variable amplitude/frequency stick shaking and a weak soft stop (stick force gradient) to provide a representative cue for the surface-mount appliqué cueing concept (described below).

The autorotation maneuvers were flown with the goal of minimizing the forward and descent velocity at landing. The desired performance goal was 10 ft/sec (or less) descent rate at ground contact, and adequate performance was 20 ft/sec (or less) descent rate at ground contact. The pilot was targeting a forward speed of 30 knots, although in general, forward speed at landing was much larger than this target value. Note that the engines were cut shortly after data logging began (which preceded slightly the rapid decrease in collective stick in the plotted results). The simulation was frozen at the moment of landing gear contact with the ground, and since data logging was not halted at this moment, this point can be seen in the simulation time histories when the logged data values maintain a constant value.

Initial evaluation results were less than favorable (the pilot started the collective pull sooner than the cue/stop motion), which prompted subsequent tuning of the collective cueing law. In terms of the collective flare law parameters, this change can be implemented by reducing the rate of control stop motion with respect to altitude (i.e., the parameter c_f in Eq. 29b). This parameter adjustment effectively translates into a reduction of the gain multiplier on the energy limit parameter (ΔE_C) in the flare cueing law formulation. Several empirical parameter adjustments were made (using Pilot B as the test pilot), and the best value was determined to be approximately 80% of the baseline value initially tested.

Figure 14 compares results before and after the modification of the collective flare cueing law. Note that both cases were flown using the soft stop cue (without stick shaking). As can be seen, the vertical descent at landing was reduced (improvement in autorotation performance), although the terminal forward velocity was increased.

An additional comparison is shown in Figure 15 that illustrates representative results contrasting Pilot A and Pilot B. Both cases shown in Figure 15 correspond to the modified collective flare cueing law. It can be seen that Pilot A and Pilot B resulted in similar terminal descent velocity, but the forward velocity at landing for Pilot B was approximately half of that for Pilot A (although the terminal pitch attitude for Pilot B was larger and likely excessive for landing). In general, it was found that Pilot B tended to wait for the collective cue, and in fact allowed the cue to directly backdrive the stick when using the soft stop cue, whereas Pilot A based the collective pull on previous flight experience. It is anticipated that improvements in Pilot A's performance could be achieved with a stronger soft stop gradient (at one point during the evaluations, Pilot A commented that stick force cue could be stronger, and correspondingly, minor adjustments were made to the force feel system with no significant impact on the overall performance observed). Clearly, one conclusion from these limited data is that implementation of the tactile cueing system will require pilot training to best use the applied tactile cues.

A summary of results from autorotation collective axis tactile cueing evaluations are provided in Table 1. This table identifies the pilot, collective axis cue type (None, SSS = strong soft stop, and SSWG = stick shaking with weak gradient), and the terminal velocity conditions (w_{final} = descent rate at landing, u_{final} = forward velocity at landing). Additional notes for the test condition are provided. Note that case numbers are not continuous due to other operational factors that negated a particular test case. Test points starting with and following Case 22, identified by "Modified collective flare law", were all performed with the updated flare law gains.

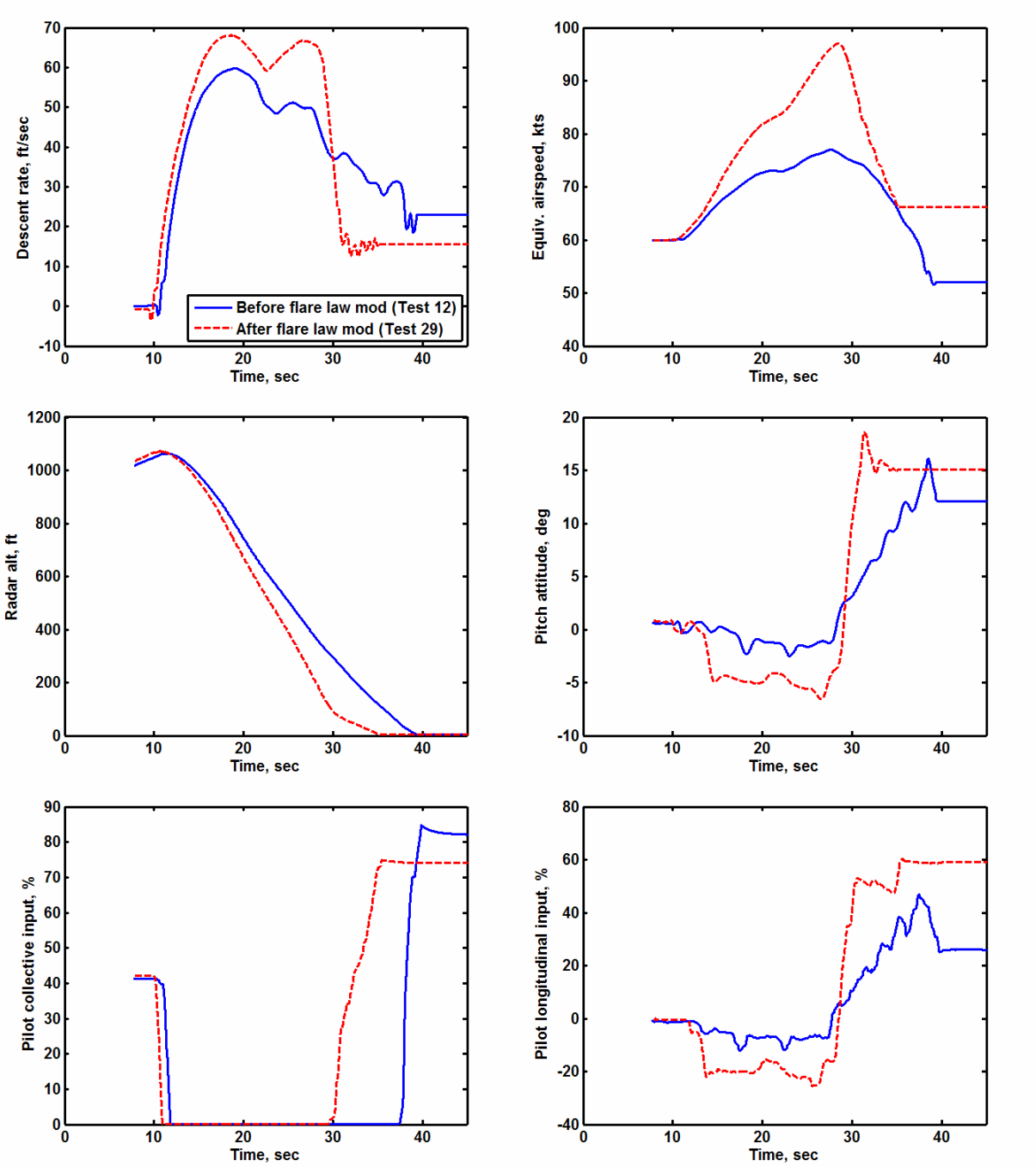

Figure 14. Representative Time Histories for Simulated Autorotation Before and After Gain Adjustment of Collective Flare Law (Pilot A)

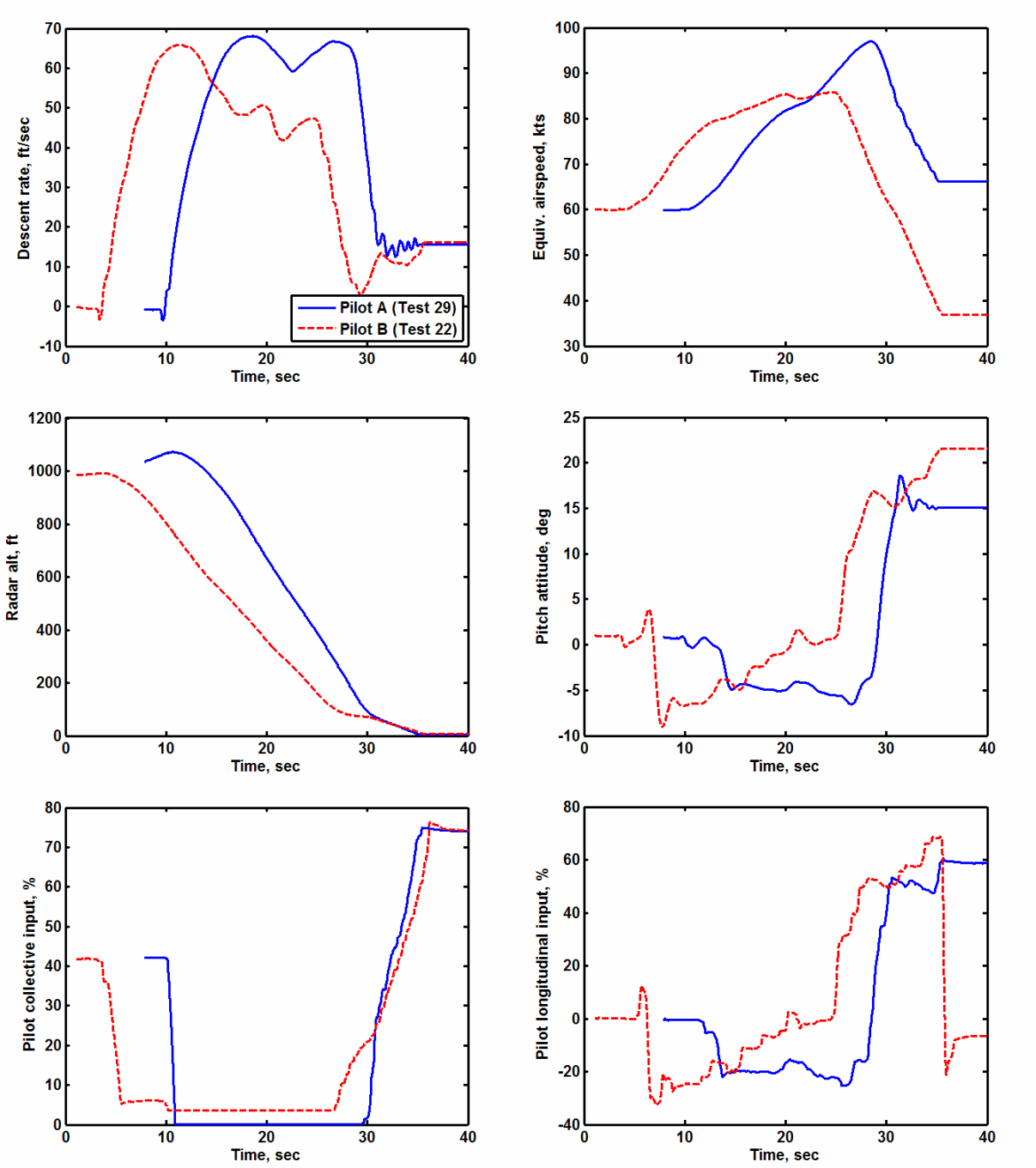

Figure 15. Representative Time Histories for Simulated Autorotation Comparing Performance of Pilot A and Pilot B with Modified Collective Axis Cueing Law

Table 1. Summary of Collective Axis Cueing Piloted Simulation Results

Case	Pilot	Collective Axis Cue	w_{final} (fpm)	u_{final} (kts)	Additional Notes
1	A	None	900	58	
4	A	None	900	60	
5	A	None	1450	62	
7	A	SSWG	1100	60	Started collective pull too early
8	A	SSWG	1750	60	w_{min} = 1000 fpm
9	A	SSS	1400	62	Did not feel cue (pulled early)
10	A	SSS	1300	50	
12	A	SSS	1400	52	Waited for cue
13	A	None	1500	43	Adjusted flare technique
14	A	None	1500	41	Adjusted flare technique
15	A	None	2950	48	Adjusted flare technique
22	B	SSS	~900	~35	Modified collective flare law
27	A	SSS	1300	59	Started collective pull too early
28	A	SSS	1850	58	RADALT callout; Started collective pull too early
29	A	SSS	950	66	RADALT callout
30	A	SSS	1650	40	RADALT callout
31	A	None	2400	62	RADALT callout
32	A	None	1550	69	RADALT callout
34	A	None	900	70	RADALT callout
35	A	SSWG	2050	43	RADALT callout; pilot felt cue and could follow
36	A	SSWG	1950	40	RADALT callout; pilot felt cue but wants to pull slower
37	A	SSWG	1450	48	RADALT callout

In summary, results suggest that the collective axis tactile cueing aided in the execution of the flare (in addition, while not discussed above, the rotor speed controller/limiting was found to provide proper corrective actions to maintain rotor speed within limits during autorotation entry). This observation is conditioned on the fact that the pilot must use the cue, which indicates that pilot training may be required. Modification to the collective flare cueing law during the piloted evaluations was also seen to improve performance, and refinements/extensions (in future work) can be expected to further enhance its implementation. In addition, it was found that both steady and unsteady cues could be perceived and interpreted by the pilot, suggesting that both methods may be viable (again accounting for sufficient pilot training). Future work focusing on more formal (i.e., handling qualities) evaluations would need to address limitations of the simulated environment to ensure that sufficient visual fidelity/cues are present to not adversely affect the simulated autorotation recovery scenarios (MTEs).

APPLIQUE TACTILE CUEING CONCEPT

As noted previously, one aspect of this research effort has been to investigate alternative cueing methods that permit the application of tactile feedback for enhancing autorotation execution (as well as general handling qualities) in "legacy" aircraft without active flight controls. To this end, initial investigation was performed to identify and test an "appliqué" device that provides tactile cues to the pilot.

Initial investigation examined a variety of tactile cueing devices, including surface mounted devices driven by smart

materials. Ultimately, it was found that an effective inceptor cueing mechanism suitable as an appliqué device was constructed from a series of standard thin-format "pager buzzer" motor having an eccentric weight mounted on its output shaft. This mechanism had several advantages including:

1. Surface-mounting of these units does not add appreciably to stick grip diameter.
2. Force output is proportional to the square of the applied voltage (through motor rpm control).
3. Cueing forces can be made large enough to be felt easily in a bare or gloved hand.
4. The frequency of excitation is sufficiently high so as not to be masked by other vibratory sources present in the helicopter.
5. The speed of response of the motor is almost instantaneous, suggesting that modulation of output force as a function of time or stick displacement is easily done.

Evaluation of appliqué device concepts was first performed in a benchtop test environment. It was found through bench testing that while the isolated vibration from the eccentric motor unit was substantial, it was diminished when hard-mounted to a control lever. In fact, bench testing of a prototype configuration (single axis cueing) resulted in a measurable vibration that had almost no directivity cues. It was determined that some means of softer suspension was required in order to maximize the vibratory "feel" transmitted to the pilot's hand. Addition of a layer of mechanical separation (see Figure 16 for a schematic representation) improved the overall response cue. Subsequent bench testing involving a single axis tracking task with opposing vibration motors (which attempt to drive the "pilot's" response to null the vibration by pushing away from the opposing source) indicated improved directional cues and improved task performance.

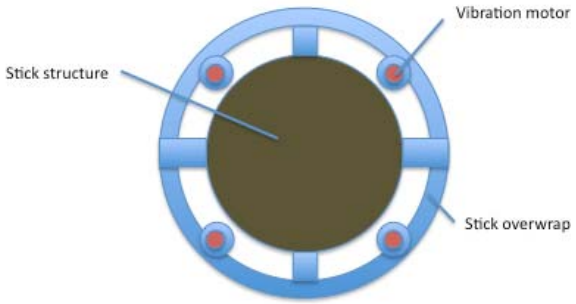

Figure 16. Illustration of Notional Mechanical Vibration Amplification Approach for Appliqué System

An important feature of an appliqué system is its ability to generate measurable force cues to the pilot in the presence of possibly substantial cabin vibration levels. To evaluate this design aspect, a representative test environment was setup to simulate (stimulate) cockpit vibrations in bench top testing and in an in-house simulation lab. In this setup, a side-stick was placed on an electrodynamic shaker that has sufficient force and excitation capability to provide representative cockpit vibration levels (representative vibration levels were estimated from cockpit measurements made as part of the Army UH-60 Airloads program).

While it was not possible to perform a full hardware-in-the-loop simulation of the appliqué device concept in a prototypical vibration environment, preliminary evaluation was performed to assess cue perception subject to vertical vibratory excitation during a representative piloting exercise. The test environment for this preliminary evaluation is shown in Figure 17. Piloted simulation testing was performed in which the appliqué device was used to cue a "hard limit" on the side-stick longitudinal and lateral displacement. Evaluations were performed with a vertical vibration level of 0.4 to 0.5 g's RMS at an excitation frequency of 20 Hz, which approximately corresponds to a 4P vibration for the H-60. Tests were performed without and with Nomex flight gloves. Results illustrating the tracking performance and limit identification are shown in Figure 18, in which the actual stick deflection is shown as the thin blue line and limits shown by the thick red box. Initial results for this appliqué tactile cueing device concept were promising, although additional testing would be required to assess its effectiveness as a cueing mechanism for autorotation safety enhancement.

Figure 17. Appliqué Device Testing in Internal Simulation Lab Setting with Simulated Vibration Background

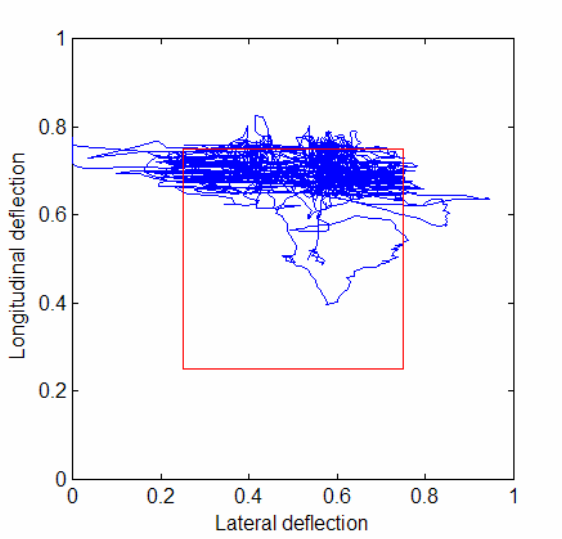

Figure 18. Appliqué Device Limit Tracking Performance from Simulation Evaluations

CONCLUSIONS

This paper describes an investigation of an autorotation tactile cueing system for improving handling qualities and enhancing safety. A cueing strategy to assist helicopter autorotation has been devised based on results from optimal trajectory analysis, and this strategy has been applied to the collective control axis. Evaluation of the collective axis autorotation guidance laws have been examined through closed-loop and piloted simulations. The following specific conclusions can be made:

1. Optimal autorotation trajectory/control analysis indicates that multiple solutions may be realized from a given entry condition that satisfy terminal velocity (landing) requirements but permit variations in the overall performance (e.g., final downrange distance traveled). Thus, providing tactile cues to track a single optimal trajectory may not be desirable for all entry conditions.
2. A rotor speed command/limiting flight control/cueing system combined with a flare cueing law, based on an integral response limit cueing design approach, provides a framework for repeatable execution of autorotation maneuvers from most entry conditions. By adopting an "envelope limiting" design strategy, greater flexibility can be provided to the pilot for autorotation execution from arbitrary entry conditions.
3. Engineering simulation evaluations indicate that the collective flare cueing law, which is based on a critical energy limit condition and mimics the optimal rotor speed profile, can be used to execute autorotation maneuvers from descent to landing.
4. A surface-mounted "appliqué" cueing device has been examined to provide tactile cues in cockpit configurations without active flight controls. Initial evaluation indicates that an electromechanical based design is more effective than other concepts in terms of force/bandwidth requirements within the design space constraints (i.e., installation on the collective/cyclic stick grip). Preliminary results involving piloted simulation testing with simulated cockpit vibrations have indicated this approach can be viable.
5. Piloted simulation evaluations of a prototype collective axis cueing system indicate that the envelope limiting cueing strategy can be used to enhance the execution of the autorotation entry and flare/landing phases provided that the cues are suitably tailored and presented to the pilot so that proper control action can be inferred and applied. Simulation evaluations examined the use of conventional soft stop/gradients and a biased stick shaker cue (to approximately represent the surface-mounted appliqué device concept), and qualitative comments from the test pilot indicate that both cues can be recognized and followed.

Results presented in this paper are from an initial feasibility study, and further work will be required to complete development and testing of a tactile cueing system for enhancing autorotation execution. Future work will focus on development and testing of a multi-axis autorotation tactile cueing system, including additional development and hardware-in-the-loop testing of appliqué tactile cueing device concepts to permit application to legacy aircraft systems. Future work will also examine formal handling qualities (HQR) evaluation of the autorotation tactile cueing system, including the development of several appropriate MTEs and performance metrics.

ACKNOWLEDGMENTS

This work was supported through an SBIR Phase I project for the U.S. Navy (Contract No. N68335-10-C-0068) with Sean Roark, Eve Ford, and Nathan Stock serving as Technical Points of Contact. The authors would also like thank Sam Evans of Penn State University for his support in this project.

REFERENCES

1. McIntyre, H. H., "A Simplified Study of High Speed Autorotation Entry Characteristics," American Helicopter Society 26th Annual Forum, Washington D.C., June 1970.
2. Johnson, W., "Helicopter Optimal Decent and Landing after Power Loss," NASA TM-73244, May 1977.
3. Lee, A. Y., Bryson, A. E., Jr., and Hindson, W. S., "Optimal Landing of a Helicopter in Autorotation," *Journal of Guidance*, Vol. 11, (1), Jan-Feb 1988.
4. Lee, A. Y., "Optimal Autorotational Descent of a Helicopter with Control and State Inequality Constraints," *Journal of Guidance*, Vol. 13, (5), Sept-Oct 1990.
5. Okuno, Y., Kawachi, K., Azuma, A., and Saito, S., "Analytical Prediction of Height-Velocity Diagram of a

Helicopter Using Optimal Control Theory," *Journal of Guidance*, Vol. 14, (2), Mar-Apr 1991.
6. Sharma, V., Zhao, Y., Chen, R. T. N., and Hindson, W. S., "Optimal OEI Clear Heliport Operation of a Multiengine Helicopter," American Helicopter Society 51st Annual Forum, Fort Worth, TX, May 1995.
7. Zhao, Y., Jhemi, A. A., and Chen, R. T. N., "Optimal Vertical Takeoff and Landing Helicopter Operation in One Engine Failure," *Journal of Aircraft*, Vol. 33, (2), Mar-Apr 1996.
8. Bottasso, C. L., Croce, A., Leonello, D., and Riviello, L., "Optimization of Critical Trajectories for Rotorcraft Vehicles," American Helicopter Society 60th Annual Forum, Baltimore, MD, June 2004.
9. Tierney, S. and Langelaan, J. W., "Autorotation Path Planning Using Backwards Reachable Set and Optimal Control," American Helicopter Society 66th Annual Forum, Phoenix, AZ, May 2010.
10. Carlson, E. B., Zhao, Y. J., and Chen, R. T. N., "Optimal Trajectories for Tiltrotor Aircraft in Total Power Failure," American Helicopter Society 54th Annual Forum, Washington D.C., May 1998.
11. Bachelder, E. N. and Aponso, B. L., "An Autorotation Flight Director for Helicopter Training," American Helicopter Society 59th Annual Forum, Phoenix, AZ, May 2003.
12. Aponso, B. L., Lee, D., and Bachelder, E. N., "Evaluation of a Rotorcraft Autorotation Training Display on a Commercial Flight Training Device," American Helicopter Society 61st Annual Forum, Grapevine, TX, 2005.
13. Howitt, J., "Carefree Maneuvering in Helicopter Flight Control," American Helicopter Society 51st Annual Forum, Fort Worth, TX, May 1995.
14. Horn, J., Calise, A. J., Prasad, J. V. R., and O'Rourke, M., "Flight Envelope Cueing on a Tiltrotor Aircraft Using Neural Network Limit Protection," American Helicopter Society 54th Annual Forum, Washington D.C., May 1998.
15. Horn, J., Calise, A. J., and Prasad, J. V. R., "Development of Envelope Protection Systems for Rotorcraft," American Helicopter Society 55th Annual Forum, Montreal, Canada, May 1999.
16. Whalley, M. S., Hindson, W. S., and Thiers, G. G., "A Comparison of Active Sidestick and Conventional Inceptors for Helicopter Flight Envelope Tactile Cueing," American Helicopter Society 56th Annual Forum, Virginia Beach, VA, May 2000.
17. Einthoven, P. G., Miller, D. G., Nicholas, J. S., and Margetich, S. J., "Tactile Cueing Experiments with a Three Axis Sidestick," American Helicopter Society 57th Annual Forum, Washington D.C., May 2001.
18. Sahasrabudhe, V., Spaulding, R., Faynberg, A., Horn, J., and Sahani, N., "Simulation Investigation of a Comprehensive Collective Axis Tactile Cueing System," American Helicopter Society 58th Annual Forum, Montreal, Canada, June 2002.
19. Binet, L., Abildgaard, M., Taghizad, A., and von Grunhagen, W., "Vortex Ring State Avoidance as Active Function on Side-sticks," American Helicopter Society 65th Annual Forum, Grapevine, TX, May 2009.
20. Whalley, M. S., Keller, J. F., Buckanin, R., and Roos, J., "Helicopter Active Control Technology Demonstrator Program," American Helicopter Society 57th Annual Forum, Washington D.C., May 2001.
21. Miller, D. G., Einthoven, P. G., Morse, C. S., and Wood, J., "HACT Flight Control System (HFCS) Control Law Overview," American Helicopter Society 58th Annual Forum, Montreal, Canada, June 2002.
22. Department of Transportation, "Rotorcraft Flying Handbook," FAA-H-8083-21, 2000.
23. Einthoven, P. G. and Miller, D. G., "The HACT Vertical Controller," American Helicopter Society 58th Annual Forum, Montreal, Canada, June 2002.
24. Horn, J. F., "Flight Envelope Limit Detection and Avoidance," Ph.D. Dissertation, Georgia Institute of Technology, May 1999.
25. Horn, J.F., Bridges, D.O., Lopes, L.V., and Brentner, K.S., "Development of a Low-Cost, Multi-Disciplinary Rotorcraft Simulation Facility," *AIAA Journal of Aerospace Computing, Information, and Communication*, Vol. 2, (7), pp. 267-284, 2005.
26. Howlett, J.J., "UH-60A Blackhawk Engineering Simulation Program: Volume I – Mathematical Model," NASA CR 166309, National Aeronautics and Space Administration, Ames Research Center, Moffett Field, CA, December 1981.
27. Horn, J.F., Bridges, D.O., Wachspress, D.A, and Rani, S.L., "Implementation of a Free-Vortex Wake Model in Real-Time Simulation of Rotorcraft," *AIAA Journal of Aerospace Computing, Information, and Communications*, Vol. 3, (3), March 2006.
28. Guo, W. and Horn, J. F., "Helicopter Flight Control with Variable Rotor Speed and Torque Limiting," American Helicopter Society 65th Annual Forum, Grapevine, TX, 2009.